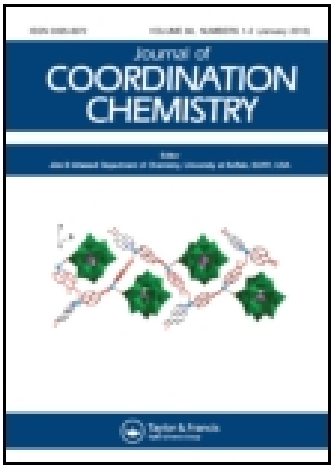

Journal of Coordination Chemistry
Publication details, including instructions for authors and subscription information:
http://www.tandfonline.com/loi/gcoo20

Two new 1-D and 3-D Wells-Dawson structures assisted by alkali metals

Ai-Xiang Tian[a], Xiao-Ling Lin[a], Na Sun[a], Yu-Jing Liu[b], Yang Yang[a] & Jun Ying[a]

[a] Department of Chemistry, Bohai University, Jinzhou, PR China

[b] Department of Chemical and Environmental Engineering, Hebei Chemical & Pharmaceutical Vocational Technology College, Shijiazhuang, PR China

Accepted author version posted online: 19 Feb 2014.Published online: 14 Mar 2014.

To cite this article: Ai-Xiang Tian, Xiao-Ling Lin, Na Sun, Yu-Jing Liu, Yang Yang & Jun Ying (2014) Two new 1-D and 3-D Wells-Dawson structures assisted by alkali metals, Journal of Coordination Chemistry, 67:3, 495-505, DOI: 10.1080/00958972.2014.895825

To link to this article: http://dx.doi.org/10.1080/00958972.2014.895825

Journal of Coordination Chemistry, 2014
Vol. 67, No. 3, 495–505, http://dx.doi.org/10.1080/00958972.2014.895825

Two new 1-D and 3-D Wells–Dawson structures assisted by alkali metals

AI-XIANG TIAN*†, XIAO-LING LIN†, NA SUN†, YU-JING LIU‡, YANG YANG† and JUN YING†

†Department of Chemistry, Bohai University, Jinzhou, PR China
‡Department of Chemical and Environmental Engineering, Hebei Chemical & Pharmaceutical Vocational Technology College, Shijiazhuang, PR China

(*Received 12 September 2013; accepted 30 October 2013*)

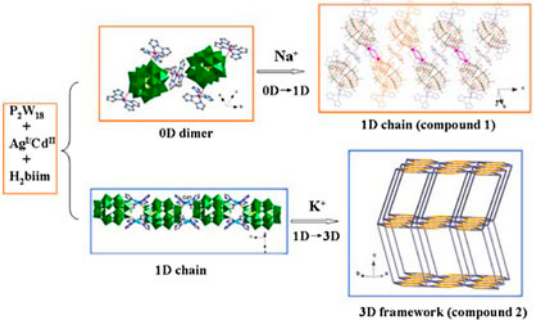

Two new Wells–Dawson based compounds containing alkali metals, $[Ag(H_2biim)_2]_2{\cdot}[Ag_5(H_2biim)_{10}Na_2(H_2O)_2(H_{3/2}P_2W_{18}O_{62})_2]{\cdot}12H_2O$ (**1**) and $[Cd(H_2biim)_2\,K(P_2W_{18}O_{62})_{1/2}]$ (**2**) (H_2biim = 2,2′-biimidazole), have been synthesized under hydrothermal conditions. In **1**, two-supporting Wells–Dawson anions are linked by a $[Ag(H_2biim)_2]^+$ subunit to form a dimer. The adjacent dimers are further connected by Na^+ through (POM)O-Na-O(POM) bonds to build a 1-D chain. In **2**, adjacent anions are linked by two $[Cd_2(H_2biim)_2]^{4+}$ subunits and a 1-D chain is formed. Furthermore, the anion in the chain is fused by six K^+ ions and a 3-D framework is obtained. The alkali metals exhibit crucial influence on the conversion of dimensionality assisting anions and Ag-H_2biim subunits to construct 1-D and 3-D frameworks. The electrochemical and photocatalytic properties of **1** and **2** have been investigated.

Keywords: Wells–Dawson polyoxometalate; Alkali metals; Hydrothermal synthesis; Electrochemical property; Photocatalytic properties

*Corresponding author. Email: tian@bhu.edu.cn

1. Introduction

Polyoxometalates (POMs) are a class of metal oxide clusters exhibiting controllable sizes/shapes [1–3] and bearing interesting physical and chemical properties such as catalysis, biochemistry, photochemistry, sorption, and magnetism [4–6]. Syntheses of POM-based inorganic–organic hybrid materials modified by transition metal complexes (TMCs) have become an attractive branch of POMs [7–9]. The POMs in this series can provide multiple potential coordination sites to link TMCs. Especially, the Wells–Dawson anion has 54 O (18 terminal O atoms and 36 μ_2-O). However, reported TMC-modified Wells–Dawson-based compounds are relatively scarce [10–12]. For example, a series of Wells–Dawson-based structures modified by TMCs have been obtained [13–15]. Thus, the syntheses of Wells–Dawson/TMCs compounds will attract more attention. Selection of organic ligands becomes a key synthetic strategy for construction of these compounds. In the reported Wells–Dawson-based structures, flexible ligands are usually chosen, while rigid organic ligands are usually based on 4,4′-bipyridine [16, 17]. In this work, we choose rigid 2,2′-biimidazole (H_2biim) cooperating with d^{10} metal ions to modify Wells–Dawson structures, aiming for formation of new structures. H_2biim has long distance of two N donors of different imidazole groups compared with bipyridine ligands, which may induce bi-nuclear subunits with strong metal–metal bonds [18, 19]. Thus, in this work, we explore the Wells–Dawson/d^{10} metal/H_2biim system aiming for construction of new TMC-modified Wells–Dawson structures.

Introduction of alkali metals in TMC-modified POM compounds is realized under common synthetic conditions [20], which usually exert their balancing charge role. However, under hydrothermal conditions alkali metals are rarely observed in POM-based compounds. There are only a few examples of this series [21, 22]. The alkali metals can play the role of linkers to connect POM anions and TMCs subunits, increasing the dimensionality of the structures. Thus, under hydrothermal conditions introduction of alkali metals to POM-based compounds becomes a challenge for forming high dimensional frameworks, especially for Wells–Dawson-based compounds. Zhou's group has reported a K-linked Wells–Dawson compound, $K_2[Ag_2(biim)_2]_2P_2W_{18}O_{62}$ (biim = biimidazole) [23], achieving the role of structural assistants for K ions to expand the dimensionality. This work inspires our synthetic strategy to use alkali metal assisting structures under hydrothermal conditions.

In this work, using rigid H_2biim as ligands and Wells–Dawson anions as inorganic building blocks, we synthesized two new 1-D and 3-D POM-based hybrid compounds containing alkali metals, $[Ag(H_2biim)_2]_2\cdot[Ag_5(H_2biim)_{10}Na_2(H_2O)_2(H_{3/2}P_2W_{18}O_{62})_2]\cdot 12H_2O$ (**1**) and $[Cd(H_2biim)_2\,K(P_2W_{18}O_{62})_{1/2}]$ (**2**) (H_2biim = 2,2′-biimidazole). The Na^+ and K^+ ions assist to realize the dimensionality 0-D→1-D for **1** and 1-D→3-D for **2**, respectively.

2. Experimental

2.1. *Materials and measurements*

All chemicals were reagent grade and used as received from commercial sources without purification. The elemental analyses (C, H, and N) were carried out on a Perkin-Elmer 240C elemental analyzer. FT-IR spectra (KBr pellets) were taken on a Varian FT-IR 640 spectrometer. Thermogravimetric (TG) analysis was carried out with a Pyris Diamond

TG/DTA instrument in flowing N_2 with a heating rate of 10 °C/min. A CHI 440 electrochemical workstation connected to a Digital-586 personal computer was used for control of the electrochemical measurements and for data collection. A conventional three-electrode system was used. A saturated calomel electrode was used as the reference electrode and a platinum wire as the counter electrode. Chemically bulk-modified carbon-paste electrodes (CPEs) of **1** and **2** were used as the working electrodes. UV/Vis absorption spectra were obtained using a SP-1900 UV/Vis spectrophotometer.

2.2. *Preparation of the compounds*

2.2.1. Synthesis of $[Ag(H_2biim)_2]_2{\cdot}[Ag_5(H_2biim)_{10}Na_2(H_2O)_2(H_{3/2}P_2W_{18}O_{62})_2]{\cdot}12H_2O$ (1). $AgNO_3$ (0.11 g, 0.65 mM), $K_6P_2W_{18}O_{62}$ (0.20 g, 0.04 mM), and H_2biim (0.035 g, 0.27 mM) were dissolved in 10 mL of distilled water. The pH of the mixture was adjusted with 1 M NaOH solution to 4.5 and then sealed into a 20 mL Teflon-lined autoclave. After heating for 4 days at 160 °C, the reactor was slowly cooled to room temperature. Red block crystals were filtered off and washed with distilled water (45% yield based on W). Anal. Calcd for $C_{84}H_{115}Ag_7Na_2N_{56}O_{138}P_4W_{36}$ (11,660): C, 8.65; H, 0.99; N, 6.73. Found: C, 8.49; H, 0.95; N, 6.85. IR data (KBr pellet, cm^{-1}): 3450(s), 1633(s), 1564(w), 1537(w), 1396(m), 1336(w), 1099(s), 967(w), 916(w), 804(m), 726(m).

2.2.2. Synthesis of $[Cd(H_2biim)_2\,K(P_2W_{18}O_{62})_{1/2}]$ (2). Compound **2** was prepared similarly to **1**, except that $CdCl_2$ (0.12 g, 0.65 mM) was used instead of $AgNO_3$. The pH was adjusted to 3.8 with 1 M HCl. Green block crystals of **2** were obtained in 36% yield (based on W). Anal. Calcd for $C_{12}H_{12}CdKN_8O_{31}PW_9$ (2601): C, 5.54; H, 0.47; N, 4.31. Found: C, 5.47; H, 0.43; N, 4.35. IR data (KBr pellet, cm^{-1}): 3439(s), 2918 (w), 1645(w), 1569(w), 1420 (m), 1362(w), 1094(s), 976(w), 912 (w), 802(w), 716(m).

2.3. *X-ray crystallographic study*

Single-crystal X-ray diffraction analyses for **1** and **2** were collected at 293 K on a Bruker Smart 1000 CCD diffractometer with Mo-Kα ($\lambda = 0.71073$ Å) by ω and θ scan mode. The structures were solved by direct methods and refined on F^2 by full-matrix least-squares using SHELXL-97 [24]. All non-hydrogen atoms were refined anisotropically. Hydrogens from C and N were placed at calculated positions. A summary of the crystallographic data and structure refinements for **1** and **2** are given in table 1. Selected bond distances (Å) and angles (°) are listed in table S1 (see online supplemental material at http://dx.doi.org/10.1080/00958972.2014.895825).

2.4. *Preparation of 1- and 2-CPE*

1 bulk-modified carbon paste electrode (**1**-CPE) was fabricated as follows: 0.01 g of **1** and 0.1 g of graphite powder were mixed and ground together by an agate mortar and pestle to achieve a uniform mixture, and then 0.18 mL paraffin oil was added with stirring. The homogenized mixture was packed into a glass tube with a 3 mm inner diameter, and the tube surface was wiped with weighing paper. Electrical contact was established with a copper rod through the back of the electrode. In a similar manner, **2**-CPE was made with **2**.

Table 1. Crystal data and structure refinements for **1** and **2**.

	1	**2**
Formula	$C_{84}H_{115}N_{56}Ag_7Na_2O_{138}P_4W_{36}$	$C_{12}H_{12}N_8CdKO_{31}PW_9$
Fw	11,660	2601
T (K)	293(2)	293(2)
Space group	$P\bar{1}$	*Cmcm*
a (Å)	14.9668(10)	21.3237(19)
b (Å)	17.3038(12)	11.9395(11)
c (Å)	21.6104(15)	31.555(3)
α (°)	79.3760(10)	90.00
β (°)	85.0480(10)	90.00
γ (°)	84.2540(10)	90.00
V (Å^3)	5459.9(6)	8033.7(13)
Z	1	8
D_c (g cm^{-3})	3.529	4.295
μ (mm^{-1})	19.622	26.423
F (0 0 0)	5133	9056
Final R_1[a], wR_2[b] [$I > 2\sigma(I)$]	0.0711, 0.2067	0.0439, 0.1227
Final R_1[a], wR_2[b] (all data)	0.1121, 0.2254	0.0552, 0.1303
GOF on F^2	1.099	1.012

[a]$R_1 = \sum \| F_o \| - \| F_c \| / \sum | F_o |$.
[b]$wR_2 = \{\sum[w(F_o^2 - F_c^2)^2] / \sum[w(F_o^2)^2]\}^{1/2}$.

3. Results and discussion

3.1. *Synthesis*

The compounds containing alkali metals as structural linkages were synthesized under classical hydrothermal conditions. The introduction of alkali metals was not just to utilize alkali salts, but is achieved through tuning pH (NaOH) for **1** and using $K_6P_2W_{18}O_{62}$ for **2**. Though the synthetic processes are similar with other P_2W_{18}/TM ligand systems without alkali metals [13, 14], the alkali metals in **1** and **2** assist in expanding the dimensionalities. The reason may rest on the synergetic effects between Wells–Dawson anions, Ag/Cd ions and H_2biim ligands.

3.2. *Description of the crystal structures*

Crystal structure analysis reveals that **1** consists of seven Ag^I ions, fourteen H_2biim ligands, two Na^I, two α-$[P_2W_{18}O_{62}]^{6-}$ (abbreviated as P_2W_{18}) and two coordinated and twelve crystal waters (figure 1). The P_2W_{18} as the inorganic building block contains two [α-A-$PW_9O_{34}]^{9-}$ units derived from α-Keggin anion by removal of a set of three corner-shared WO_6 octahedra. The P–O and W–O bond lengths are in normal ranges [12]. Bond valence sum calculations [25] show that all W are in + VI oxidation state and all Ag are in + I oxidation state.

In **1**, there are four crystallographically independent Ag^I ions. Ag1 and Ag3 are five-coordinate by one O from one P_2W_{18} anion and four N from two H_2biim in a trigonal bipyramidal geometry, having τ values of 0.21 for Ag1 and 0.01 for Ag3 [$\tau = (\beta - \alpha)/60$] [26], with the angles N7–Ag1–N3, 174.7° (β), N1–Ag1–N5, 161.9° (α for Ag1 and N17–Ag1–N15, 165.5° (β), N13–Ag1–N19, 164.8° (α) for Ag3. The bond distances and angles around Ag1 and Ag3 are 1.97(2)–2.05(2) Å for Ag–N, 2.205(16) and 2.342(16) Å for Ag–O, 80.9 (9)°–174.7(9)° for N–Ag–N, 90.1(8)° and 107.94(8)° for N–Ag–O. Ag2 exhibits distorted

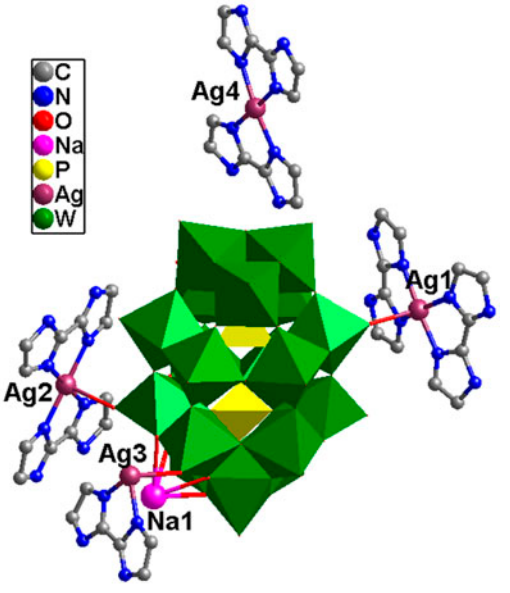

Figure 1. Polyhedron and ball/stick view of the basic crystallographic unit of **1**. The hydrogens are omitted for clarity.

octahedral geometry six-coordinate by two O from two P_2W_{18} anions and four N from two H_2biim. The bond distances and angles around Ag2 are 2.02(2) and 2.05(2) Å for Ag–N, 2.48(17) Å for Ag–O, 82.7(9)°–180.0(11)° for N–Ag–N, and 88.8(8)°–91.2(8)° for N–Ag–O. Ag4 is four-coordinate by four N from two H_2biim as a discrete $[Ag(H_2biim)]^+$ subunit. The bond distances and angles around Ag4 are 1.96(2) and 2.03(2) Å for Ag–N and 82.8(9)°–177.0(10)° for N–Ag–N. The bond distances and angles of Ag in **1** are similar to those in the four-, five-, and six-coordinate Ag^I complexes [12, 18]. In **1**, H_2biim adopts a single chelate coordination mode.

In **1**, the Wells–Dawson anion offers two asymmetric terminal oxygens (O32 and O57) to link two $[Ag(H_2biim)]^+$ (Ag1 and Ag3) subunits, forming a two-supporting anion. Two adjacent two-supporting anions are fused by a $[Ag2(H_2biim)]^+$ subunit through O55–Ag2–O55 bonds to construct a dimer, as shown in figure 2. The structure of **1** rests on joining of Na^I ions, which link two anions in different dimers in a head to head style; the anion is capped by one Na^I to connect another capped anion through two O1 W bridges. The Na^I is six-coordinate by four bridging O from one anion and two O1 W with Na–O distances of 2.39(5)−2.81(8) Å (figure S1). Introduction of Na^I ions induces the 1-D chain of **1** (figure 3), realizing the dimensionality from 0-D to 1-D. The discrete $[Ag4(H_2biim)]^+$ subunits disperse these chains balancing the charge (figure S2).

Crystal structure analysis reveals that **2** consists of one Cd^{II}, two H_2biim, 1/2 P_2W_{18} anion, and one K^I (figure 4). The P–O and W–O bond lengths are in normal ranges. Bond valence sum calculations [25] show that all W are + VI and all Cd are + II.

In **2**, there is one crystallographically independent Cd^{II}, which is four-coordinate with two N from two H_2biim, one O from one P_2W_{18} anion and one Cd1 ion in a "seesaw" geometry. The bond distances around Cd1 are 1.899(15) and 1.890 (14) Å for Cd–N, 2.732 (8) Å for Cd–O, and 2.651(5) Å for Cd1–Cd1. The strong Cd–Cd bond is unusual in POM-

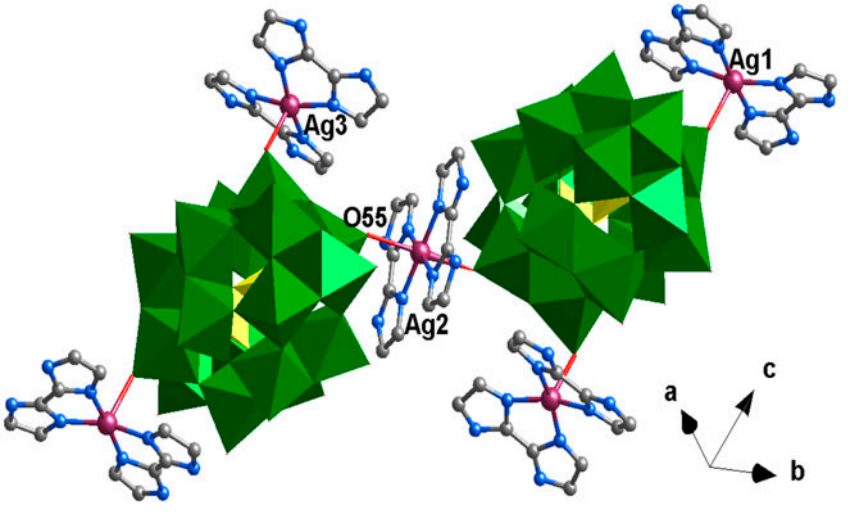

Figure 2. Two adjacent two-supporting anions are linked by Ag2 subunits to form a dimer in **1**.

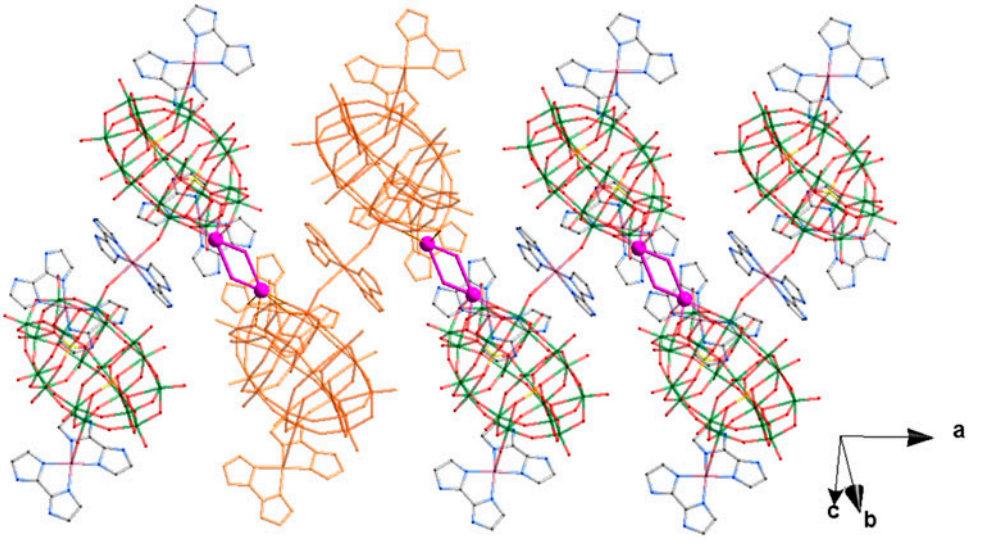

Figure 3. The dimers are connected by Na^{I} ions through Na–O1 W–Na (purple) to form a 1-D chain of **1**.

based compounds. In **2**, H_2biim utilizes two N donors in different imidazoles to link two Cd ions containing a Cd–Cd bond, induced by the longer distance of these two N donors. Coordination of H_2biim is different than that in **1**.

In **2**, pairs of $[Cd_2(H_2biim)_2]^{4+}$ subunits as bridges connect P_2W_{18} anions to form a 1-D chain (figure 5). Thus, the P_2W_{18} and Cd-H_2biim subunits only construct a 1-D structure. K^{I} ions join this system, coordinating with six O from three P_2W_{18} anions. Each P_2W_{18} anion offers 12 terminal O all from its "belts" positions to fuse six K ions (figure S3). Thus,

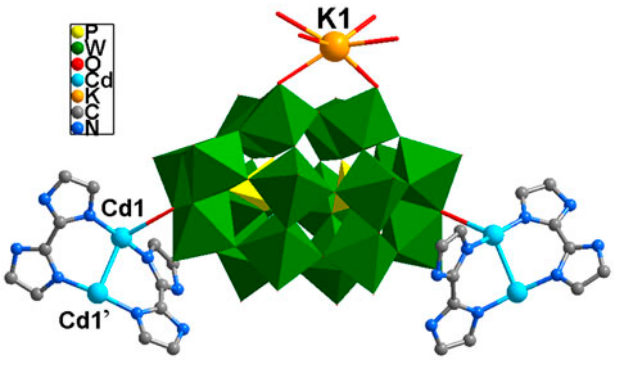

Figure 4. Polyhedron and ball/stick view of the basic crystallographic unit of **2**. The hydrogens are omitted for clarity.

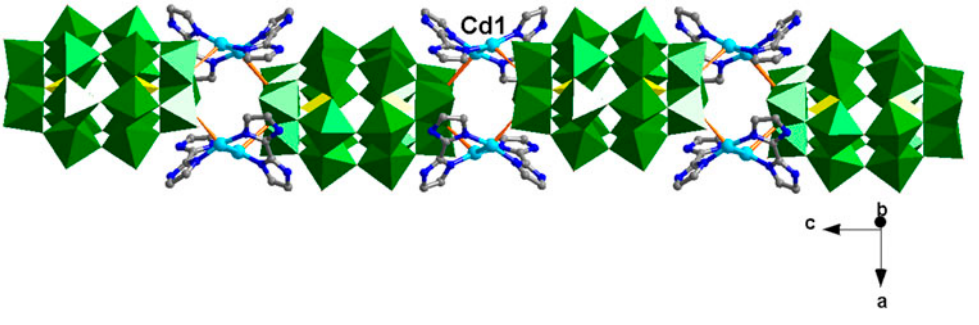

Figure 5. The 1-D chain of P_2W_{18} anions linked by pairs of $[Cd_2(H_2biim)_2]^{4+}$ subunits in **2**.

these 1-D chains are linked by K ions to build a 3-D framework of **2** (figures 6 and S4). K ions assist the P_2W_{18}-Cd-H_2biim 1-D chain to construct a 3-D structure, realizing the dimensionality increase.

3.3. *FT-IR spectra*

IR spectra of **1** and **2** are shown in figure S5. Bands at 1099, 967, 916, and 804 cm^{-1} for **1** and 1094, 976, 912, and 802 cm^{-1} for **2** are attributed to ν(P–O), ν(W=O), and ν(W–O–W), respectively [27]. Furthermore, bands at 1633−1336 cm^{-1} for **1** and 1645−1362 cm^{-1} for **2** are attributed to H_2biim.

3.4. *Electrochemical properties*

The electrochemical behaviors of **1**- and **2**-CPEs are studied. Owing to the similarity, the **1**-CPE has been taken as an example to study their electrochemical properties. The cyclic voltammograms for **1**-CPE in 0.1 M H_2SO_4 + 0.5 M Na_2SO_4 aqueous solution at different scan rates are presented in figure 7 in the potential range from + 250 to –750 mV. There exist three reversible redox peaks I–I′, II–II′, and III–III′ with the half-wave potentials

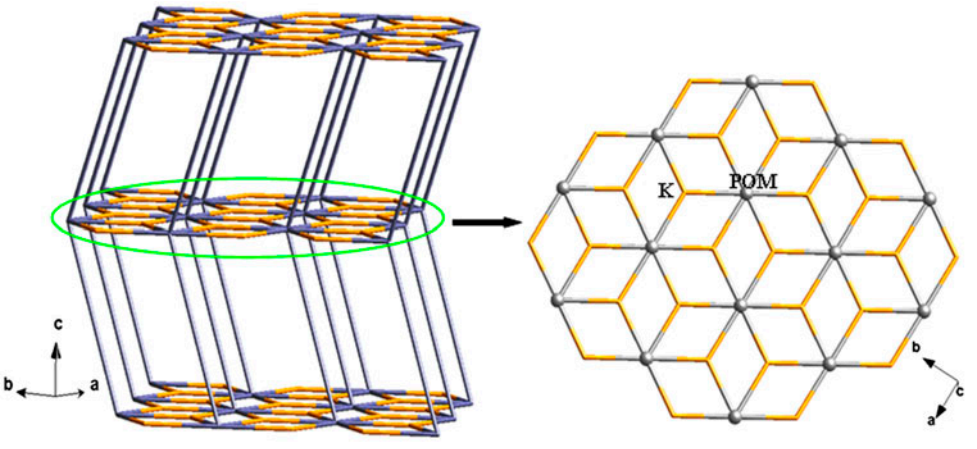

Figure 6. Left: The schematic view of the 3-D framework of **2**. Right: P_2W_{18} anions are linked by K ions to construct a 2-D inorganic layer.

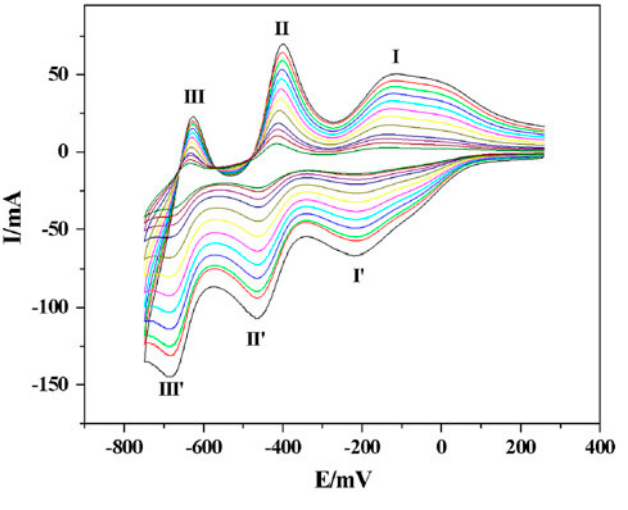

Figure 7. Cyclic voltammograms of **1**-CPE in a 0.1 M H_2SO_4 + 0.5 M Na_2SO_4 aqueous solution at different scan rates (from inner to outer: 40, 60, 80, 100, 150, 200, 250, 300, 350, 400, 450, and 500 mV s^{-1}).

$E_{1/2}$ = $(E_{pa} + E_{pc})/2$ at –185(I–I′), –436(II–II′), and –656 (III–III′) mV (scan rate: 100 mV s^{-1}). The redox peaks I–I′, II–II′, and III–III′ correspond to three consecutive two-electron processes of the W centers [10, 28]. The peak potentials change gradually following the scan rates from 40 to 500 mV s^{-1}: the cathodic peak potentials shift to the negative direction and the corresponding anodic peak potentials shift to the positive direction with increasing scan rates. The peak currents are proportional to the scan rates (figure S6), indicating that the redox process of **1**-CPE is surface-controlled.

The electrocatalytic reduction of nitrite in 0.1 M H_2SO_4 + 0.5 M Na_2SO_4 aqueous solution was investigated at **1**-CPE, as shown in figure 8. With addition of nitrite, all three reduction

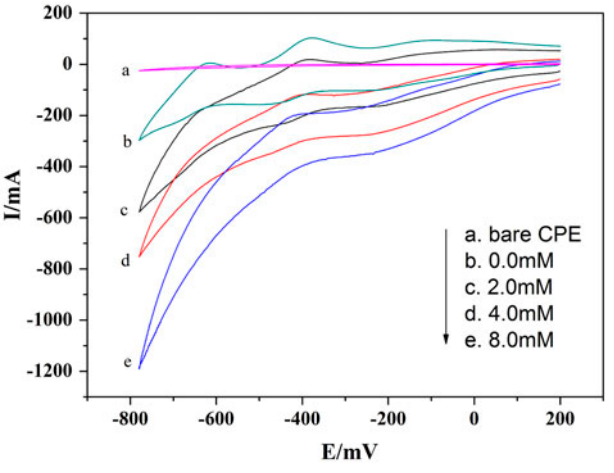

Figure 8. Cyclic voltammograms of a bare CPE in a 4.0 mM KNO_2 + 0.1 M H_2SO_4 + 0.5 M Na_2SO_4 aqueous solution (a) and **1**-CPE in a 0.1 M H_2SO_4 + 0.5 M Na_2SO_4 aqueous solution containing 0.0−8.0 mM KNO_2 (b–e). Scan rate: 100 mV s^{-1}.

peak currents increase while the corresponding oxidation peak currents decrease, suggesting that nitrite is reduced by two-, four-, and six-electron reduced species of P_2W_{18} anions. These three reduced species all show good electrocatalytic activity toward the reduction of nitrite.

3.5. *Thermogravimetric analysis*

The TGA experiments of **1** and **2** were performed under N_2 with a heating rate of 10 °C/min from 15 to 900 °C, as shown in figure S7. There are two weight loss steps of **1**. The first occurs between 15 and 150 °C corresponding to the loss of water 2.12% (Calcd 2.16%). The second weight loss step from 350 to 900 °C can be attributed to loss of H_2biim 15.95% (Calcd 16.09%). For **2**, there is only one obvious weight loss step, attributed to loss of H_2biim 10.25% (Calcd 10.30%).

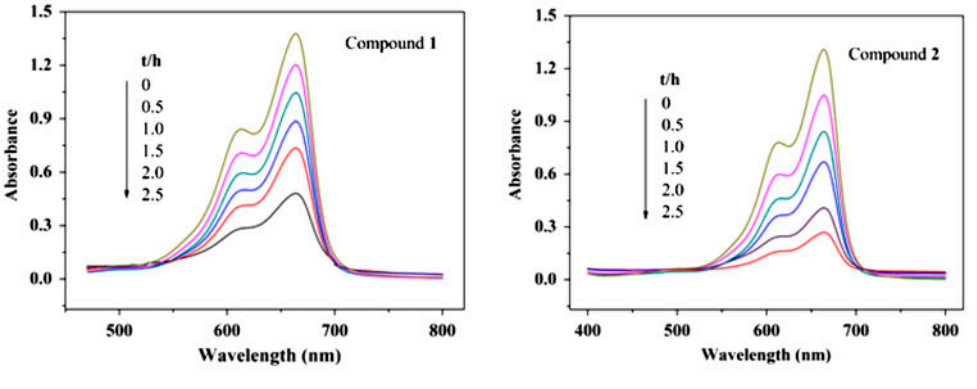

Figure 9. Absorption spectra of the MB solution during the decomposition reaction under UV light irradiation with the use of **1** and **2**.

3.6. *Photocatalytic properties*

The photocatalytic properties of **1** and **2** were investigated in methylene blue (MB) solution ($10.0\,mg\,L^{-1}$) under UV irradiation from a Hg lamp (figure 9). Absorbance of MB decreases from 1.38 to 0.47 for **1** and 1.31 to 0.27 for **2** after 2.5 h; the conversions of MB are 66% for **1** and 79% for **2** after 2.5 h. These results suggest that **1** and **2** may be photocatalysts with photocatalytic activities in the reduction of some organic dyes.

4. Conclusion

Two new Wells–Dawson based inorganic–organic hybrid materials have been synthesized under hydrothermal conditions utilizing rigid H_2biim ligands. The alkali metals are introduced to these two structures, assisting to increase the dimensionality from 0-D to 1-D for **1** and 1-D to 3-D for **2**. In **1**, the anions and Ag-H_2biim subunits construct a dimer. The Na ions bridge adjacent dimers to form a wave-like chain. In **2**, the anions are linked by a pair of $[Cd_2(H_2biim)_2]^{4+}$ subunits to build a 1-D chain. K ions bridge these chains through coordinating with P_2W_{18} anions to form a 3-D framework. The introduction of Na and K ions to increase dimensionality is scarce, especially utilizing hydrothermal techniques. Further study on the introduction of other alkali metals as linkers is underway.

Supplementary material

Crystallographic data for the structures reported in this article have been deposited in the Cambridge Crystallographic Data Center with CCDC Number 939152 for **1** and 939153 for **2**.

Funding

This work was supported by the National Natural Science Foundation of China [grant numbers 21101015, 21171025, and 21201021]; the Program for New Century Excellent Talents in University [NCET-09-0853]; the Program of Innovative Research Team in University of Liaoning Province [LT2012020]; Doctoral Initiation Project [grant number 20111147] of Liaoning Province and Talent-supporting Program Foundation of Education Office of Liaoning Province [LJQ2012097].

References

[1] F.J. Ma, S.X. Liu, C.Y. Sun, D.D. Liang, G.J. Ren, F. Wei, Y.G. Chen, Z.M. Su. *J. Am. Chem. Soc.*, **133**, 4178 (2011).
[2] H.N. Miras, C.J. Richmond, D.L. Long, L. Cronin. *J. Am. Chem. Soc.*, **134**, 3816 (2012).
[3] P. Huang, C. Qin, Z.M. Su, Y. Xing, X.L. Wang, K.Z. Shao, Y.Q. Lan, E.B. Wang. *J. Am. Chem. Soc.*, **134**, 14004 (2012).
[4] H. Bai, N. Su, W.T. Li, X. Zhang, Y. Yan, P. Li, S.X. Ouyang, J.H. Ye, G.C. Xi. *J. Mater. Chem. A*, **1**, 6125 (2013).
[5] L. Wang, B.B. Zhou, K. Yu, Z.H. Su, S. Gao, L.L. Chu, J.R. Liu, G.Y. Yang. *Inorg. Chem.*, **52**, 5119 (2013).
[6] D. Liu, Y. Lu, H.Q. Tan, W.L. Chen, Z.M. Zhang, Y.G. Li, E.B. Wang. *Chem. Commun.*, **49**, 3673 (2013).

[7] C. Zou, Z.J. Zhang, X. Xu, Q.H. Gong, J. Li, C.D. Wu. *J. Am. Chem. Soc.*, **134**, 87 (2012).
[8] X.L. Wang, Y.F. Bi, B.K. Chen, H.Y. Lin, G.C. Liu. *Inorg. Chem.*, **7**, 2443 (2008).
[9] X.Y. Wu, Q.K. Zhang, X.F. Kuang, W.B. Yang, R.M. Yu, C.Z. Lu. *Dalton Trans.*, 11783 (2012).
[10] A.X. Tian, J. Ying, J. Peng, J.Q. Sha, Z.G. Han, J.F. Ma, Z.M. Su, N.H. Hu, H.Q. Jia. *Inorg. Chem.*, **47**, 3274 (2008).
[11] C.D. Zhang, S.X. Liu, C.Y. Sun, F.J. Ma, Z.M. Su. *Cryst. Growth Des.*, **9**, 3655 (2009).
[12] M. Zhu, S.Q. Su, X.Z. Song, Z.M. Hao, S.Y. Song, H.J. Zhang. *CrystEngComm*, **14**, 6452 (2012).
[13] C. Liang, Y. Lu, H. Fu, W.L. Chen, E.B. Wang. *J. Coord. Chem.*, **65**, 3254 (2012).
[14] S. Yao, J.H. Yan, Y.C. Yu, E.B. Wang. *J. Coord. Chem.*, **65**, 1451 (2012).
[15] Y.L. Xu, K. Yu, B.B. Zhou, Z.H. Su, J. Wu. *J. Coord. Chem.*, **66**, 1303 (2013).
[16] J.Q. Sha, J. Peng, Y.Q. Lan, Z.M. Su, H.J. Pang, A.X. Tian, P.P. Zhang, M. Zhu. *Inorg. Chem.*, **47**, 5145 (2008).
[17] J.Q. Sha, C. Wang, J. Peng, J. Chen, A.X. Tian, P.P. Zhang. *Inorg. Chem. Commun.*, **10**, 1321 (2007).
[18] P.P. Zhang, J. Peng, H.J. Pang, J.Q. Sha, M. Zhu, D.D. Wang, M.G. Liu. *CrystEngComm*, **13**, 3832 (2011).
[19] C.L. Meng, P.P. Zhang, J. Peng, X. Wang, Y. Shen, M.G. Liu, D.D. Wang, K. Alimaje. *J. Cluster Sci.*, **23**, 567 (2012).
[20] H. Liu, C. Qin, Y.G. Wei, L. Xu, G.G. Gao, F.Y. Li, X.S. Qu. *Inorg. Chem.*, **47**, 4166 (2008).
[21] S. Chang, C. Qin, E.B. Wang, Y.G. Li, X.L. Wang. *Inorg. Chem. Commun.*, **9**, 727 (2006).
[22] J.Q. Sha, J. Peng, J. Chen, H.S. Liu, A.X. Tian, P.P. Zhang. *Solid State Sci.*, **9**, 1012 (2007).
[23] Y.L. Xu, B.B. Zhou, Z.H. Su, K. Yu, J. Wu. *J. Coord. Chem.*, **64**, 3670 (2011).
[24] G.M. Sheldrick. *Acta Crystallogr. Sect. A: Found. Crystallogr.*, **64**, 112 (2008).
[25] I.D. Brown, D. Altermatt. *Acta Crystallogr. Sect. B: Struct. Sci.*, **41**, 244 (1985).
[26] A.W. Addison, T.N. Rao. *J. Chem. Soc., Dalton Trans.*, 1349 (1984).
[27] H.X. Yang, S.P. Guo, J. Tao, J.X. Lin, R. Cao. *Cryst. Growth Des.*, **9**, 4735 (2009).
[28] M. Sadakane, E. Steckhan. *Chem. Rev.*, **98**, 219 (1998).